

**Supplemental Tables and Figures for:**  
**WNT1 Inducible Signaling Pathway Protein 1 (WISP1/CCN4) stimulates melanoma cell invasion and metastasis by promoting epithelial – mesenchymal transition**

Wentao Deng<sup>1,2</sup>, Audry Fernandez<sup>1,2</sup>, Sarah L. McLaughlin<sup>2,3</sup>, and David J. Klink II<sup>1,2,4\*</sup>

<sup>1</sup>Department of Microbiology, Immunology and Cell Biology, West Virginia University, Morgantown, WV 26505, USA;

<sup>2</sup>WVU Cancer Institute, West Virginia University, Morgantown, WV 26505, USA;

<sup>3</sup>Animal Models and Imaging Facility, West Virginia University, Morgantown, WV 26505, USA;

<sup>4</sup>Department of Chemical and Biomedical Engineering, West Virginia University, Morgantown, WV 26505, USA.

**Contents:**

Supplementary Table S1. Summary of mutation rate that includes both changes in single nucleotides and in copy numbers for TCGA melanoma (SKCM) samples from where both types of mutational data are reported.

Supplementary Table S2. WISP1 secretion from different cell lines cultured in 2D.

Supplementary Table S3. Densitometry measurement of protein levels in Fig. 7.

Supplementary Figure S1. High resolution version of Fig.3B.

Supplementary Figure S2. High resolution version of Fig.3D

Supplementary Figure S3. High resolution version of Fig.3F.

Supplementary Figure S4. High resolution version of Fig.3H

Supplementary Figure S5. Liver metastasis in experimental metastasis assay using C57BL/6Ncr1 mice with B16F10 and its knockout cells.

Supplementary Figure S6. Real time genomic qPCR revealed that Wisp1 knockout repressed the spontaneous metastasis of melanoma cell line B16F10 in C57BL/6Ncr1 mice.

Supplementary Figure S7. High resolution version of Fig.4B.

Supplementary Figure S8. High resolution version of Fig.4F.

Supplementary Figure S9. High resolution version of Fig.6E.

**Supplementary Table S1.** Summary of mutation rate that includes both changes in single nucleotides and in copy numbers for TCGA melanoma (SKCM) samples from where both types of mutational data are reported.

Gene	Melanoma samples with Single Nucleotide Variant (SNV) and Copy Number Variant (CNV) data (N=287)		Q-value for CNV
	Rate	Type	
<b>NRAS</b>	30%	87 SNV 8 Amplification	9.79E-07
<b>BRAF</b>	51%	143 SNV 18 Amplification	1.64E-07
<b>PTEN</b>	15%	25 SNV 19 Deletion	1.85E-27
<b>TP53</b>	17%	48 SNV 3 Deletion	3.69E-02
<b>CDKN2A</b>	43%	40 SNV 1 Amp 88 Del	<1.0e-30
<b>CTNNB1</b>	7%	16 SNV 3 Amplification	1.39E-01
<b>MITF</b>	8%	6 SNV 19 Amplification	2.27E-13
<b>KIT</b>	7%	12 SNV 10 Amplification	2.39E-03
<b>WISP1</b>	8%	7 SNV 16 Amplification	2.90E-05

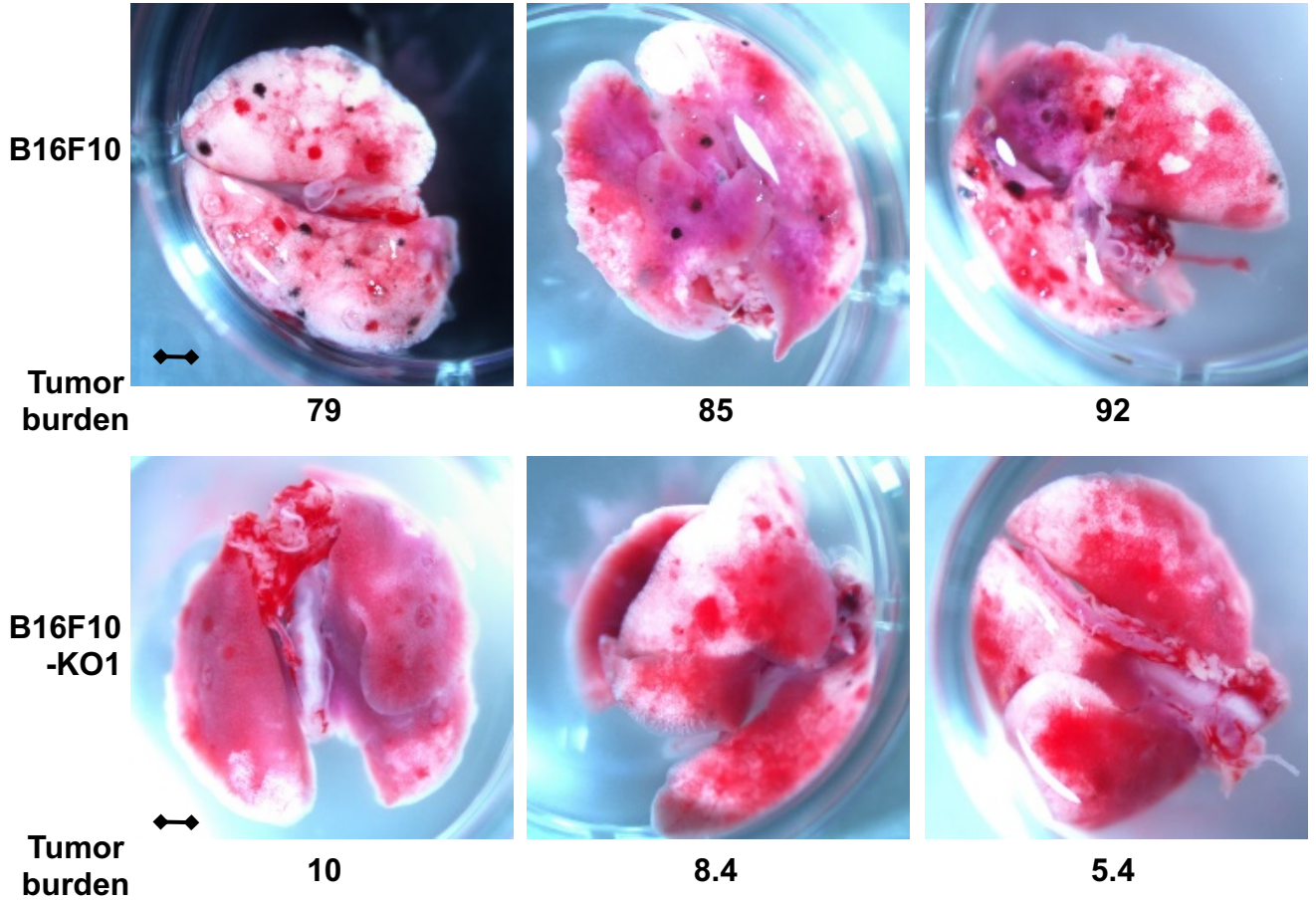
Gene mutation statistics from indicated numbers of cutaneous melanoma samples (SKCM) was obtained from the Cancer Genome Atlas (TCGA) through cBioPortal (retrieved 09/24/2018 - 52,53). Q-value corresponds to the probability of the observed or more extreme copy number variant is explained by random chance, where the value has been adjusted using the Benjamini and Hochberg FDR correction.

**Supplementary Table S2.** WISP1 secretion from different cell lines cultured in 2D.

Cell	CONC (pg/ml)	Cell	CONC (pg/ml)
B16F0	605 ± 15	B16F10-KO1	n.d.
B16F10	1,300 ± 35	B16F10-KO2	n.d.
E0771	< 20	B16F10-KO1-pBabe	n.d.
LLC1	< 20	B16F10-KO1-hSnai1	n.d.
Melan-A	1018 ± 32	B16F10-KO1-mWisp1	3465 ± 233
NIH3T3	83 ± 2.2	NIH3T3-KO	n.d.
YUMM1.1	< 20	NIH3T3-pBabe	90.3 ± 2.8
YUMM1.7	451 ± 25	NIH3T3-mWisp1	920 ± 15.6
RPMI-7951	1,331 ± 34	YUMM1.7-KO1	n.d.
SK-MEL-3	n.d.	YUMM1.7-KO2	n.d.
SK-MEL-24	n.d.	RPMI-7951-KO1	n.d.
SH-4	n.d.	RPMI-7951-KO2	n.d.

Relative WISP1 concentration (CONC), presented as mean with standard error, was determined for 48-hour conditioned medium of each cell line plated at a similar confluence with ELISA using human recombinant WISP1 as standard. n.d., not detected.

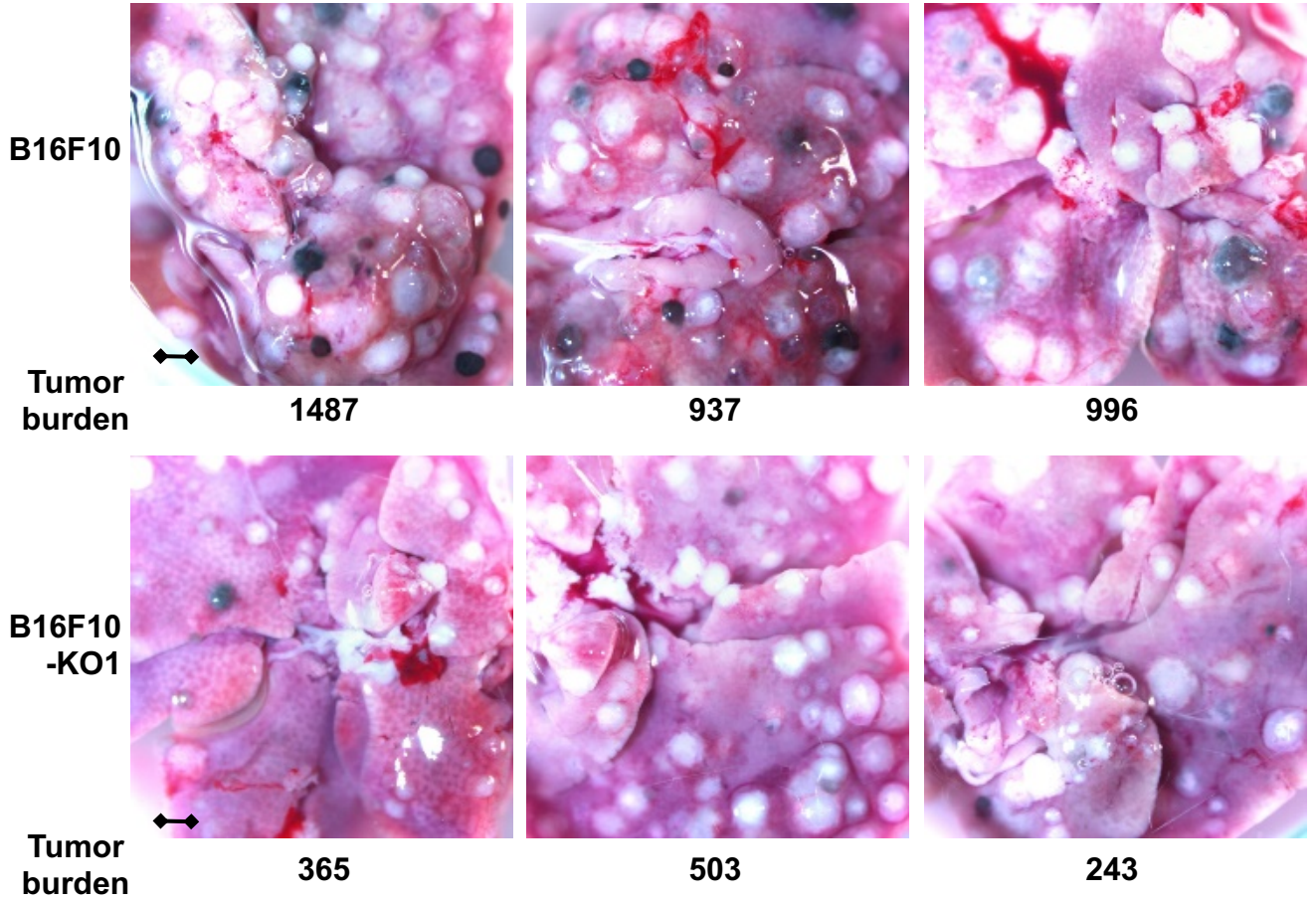
**Lung Metastasis in NSG Mice**



Scale bar: 2mm; Tumor load: tumor cells in 10<sup>4</sup> lung cells

**Supplementary Figure S1.** High resolution version of Fig.3B.

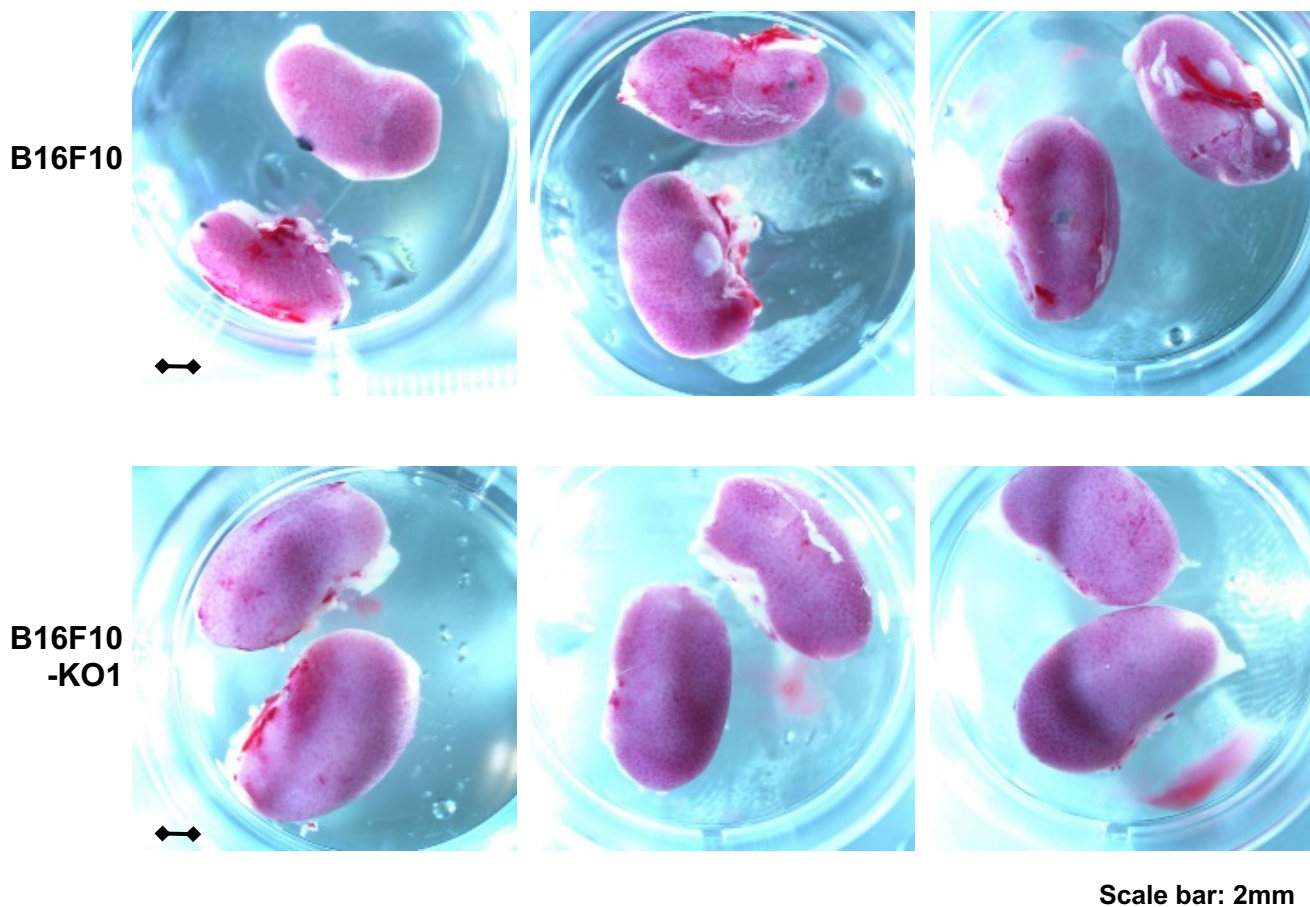
**Liver Metastasis in NSG Mice**



Scale bar: 2mm; Tumor load: tumor cells in  $10^4$  lung cells

**Supplementary Figure S2.** High resolution version of Fig.3D.

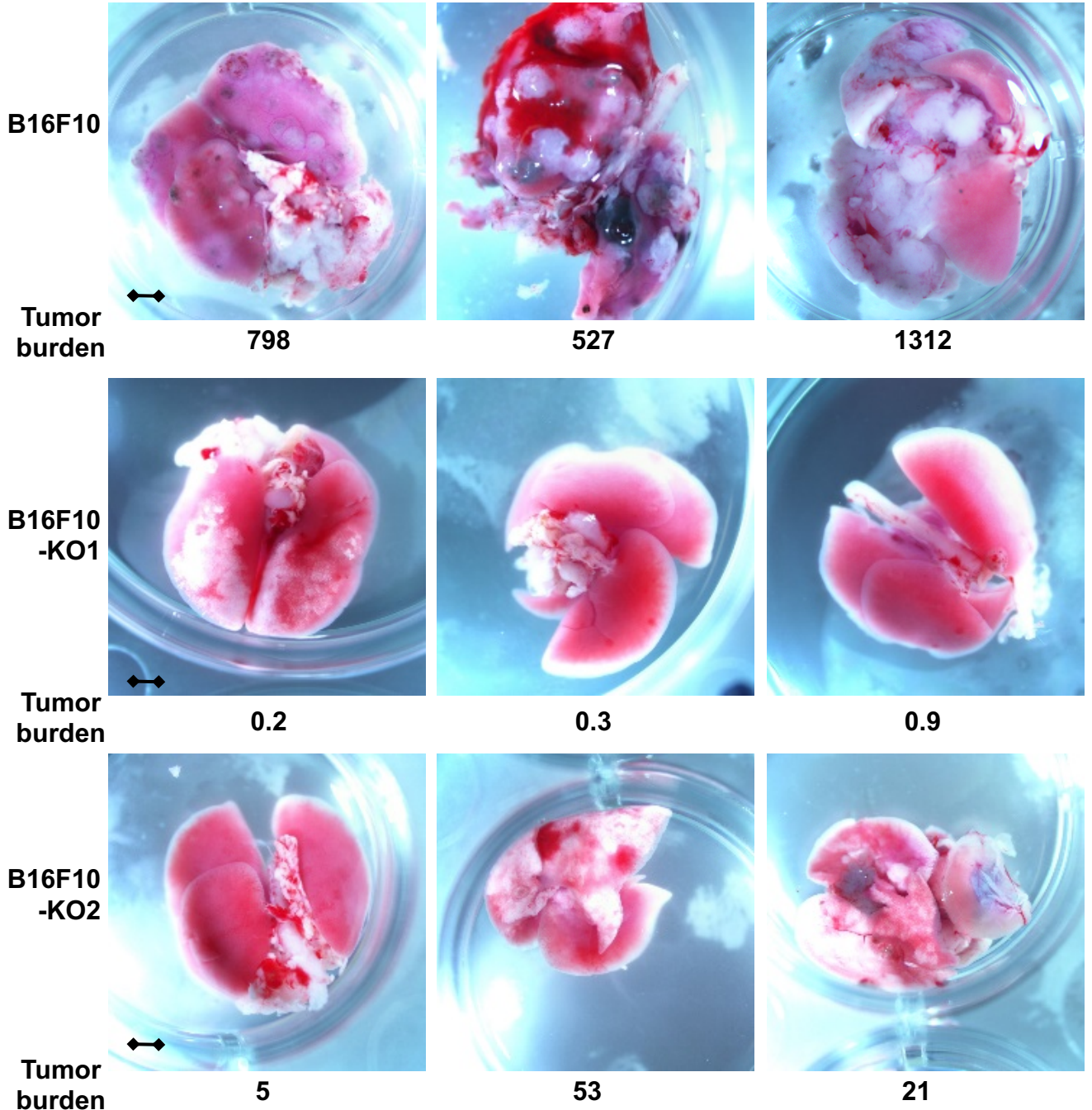
## Kidney Metastasis in NSG Mice



**Supplementary Figure S3.** High resolution version of Fig.3F.

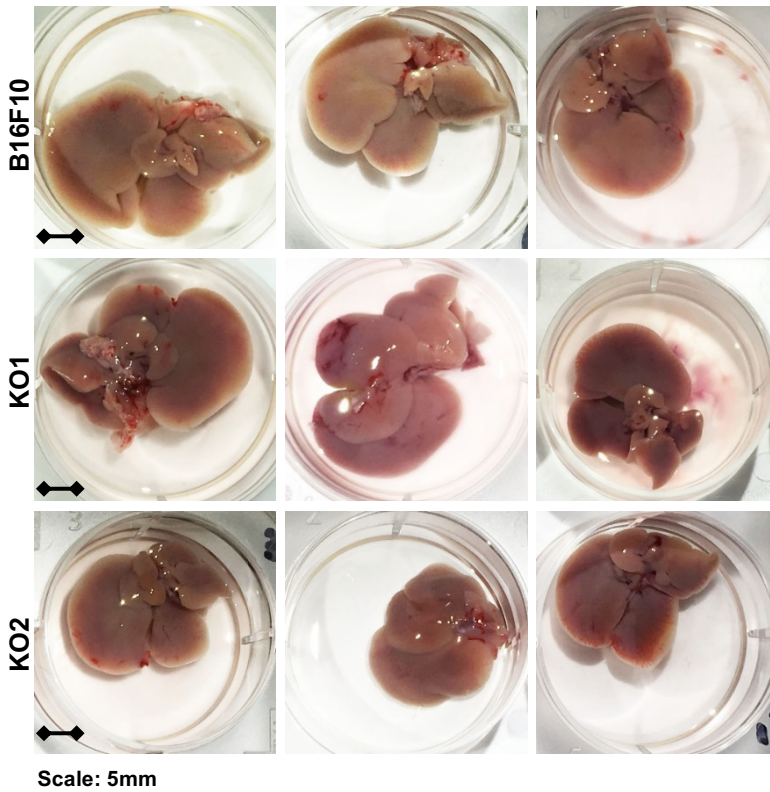
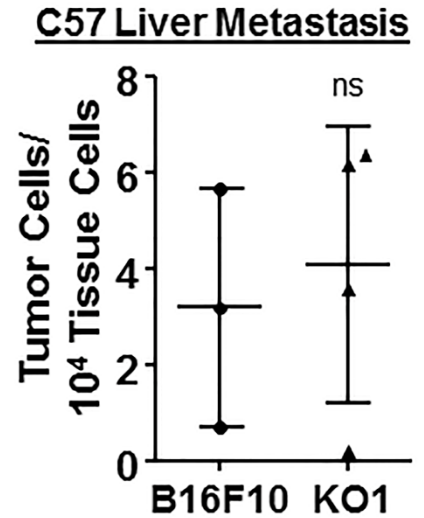


## Lung Metastasis in C57 Mice



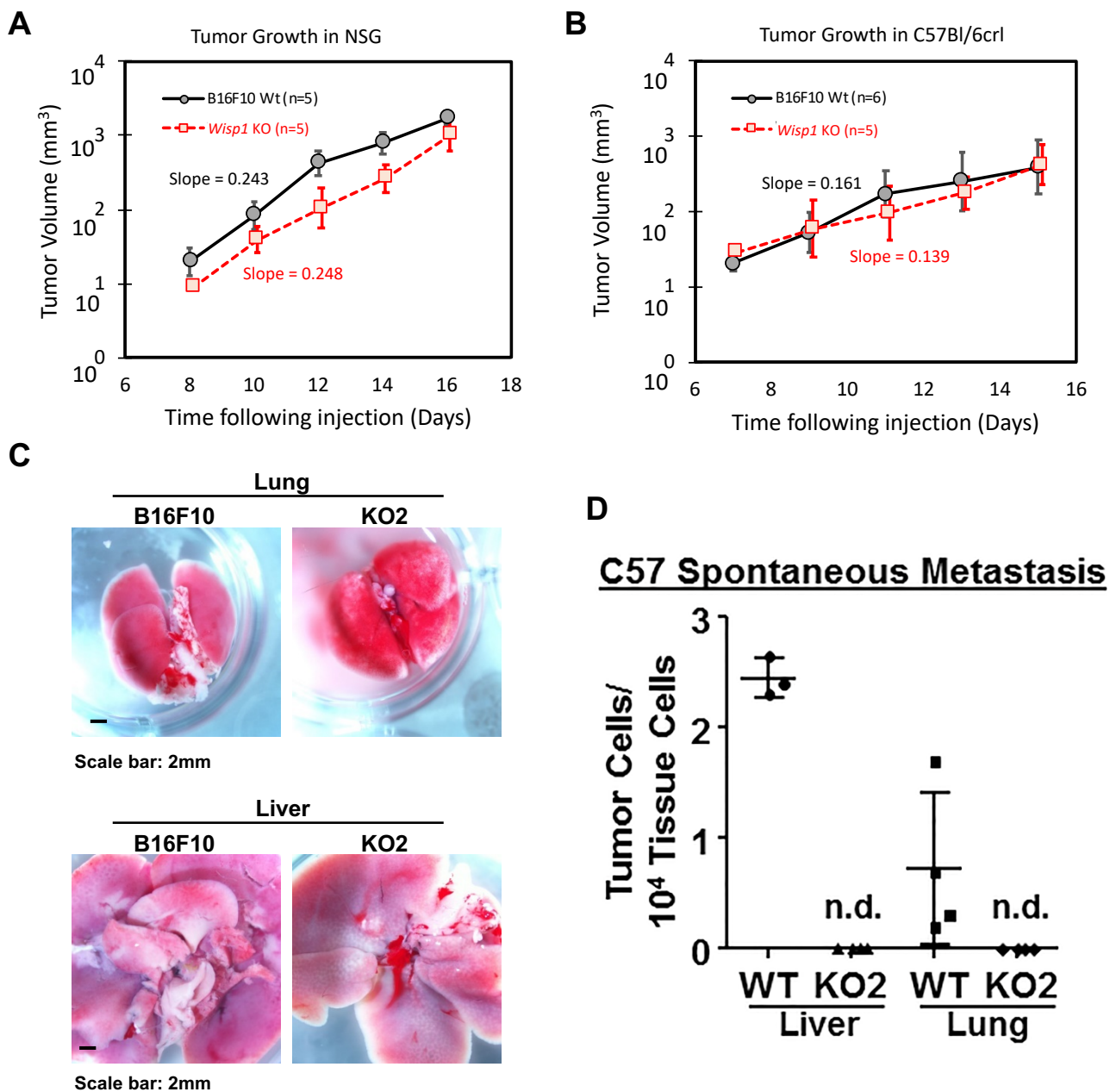
Scale bar: 2mm; Tumor load: tumor cells in  $10^4$  lung cells

Supplementary Figure S4. High resolution version of Fig.3H.

**A****B**

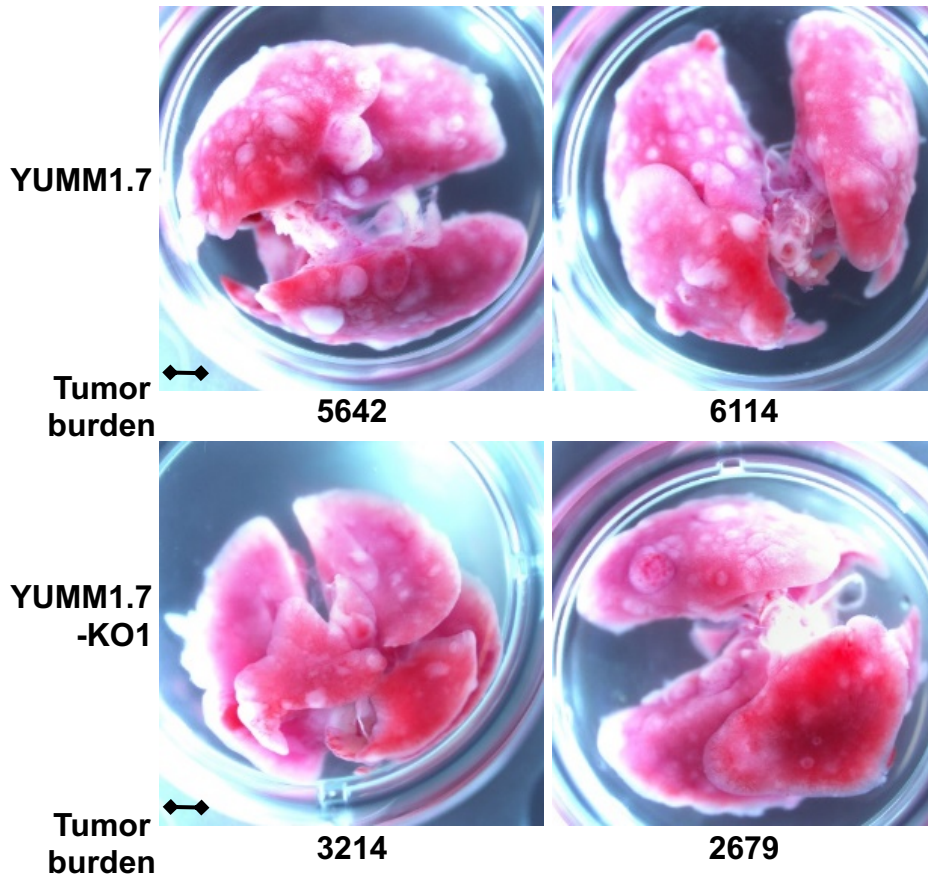
**Supplementary Figure S5.** Liver metastasis in experimental metastasis assay using C57BL/6Ncr1 mice with B16F10 and its knockout cells. (A) Representative livers from C57BL/6Ncr1 mice with B16F10 or knockout cells (-KO1 and -KO2) in experimental metastasis assay (Fig. 3G-3I). (B) Real time genomic qPCR quantitatively comparing tumor liver metastatic burdens (tumor cell number within 10,000 mouse tissue cells). ns, not significant.





**Supplementary Figure S6.** Real time genomic qPCR revealed that *Wisp1* knockout repressed the spontaneous metastasis of melanoma cell line B16F10 in C57BL/6Ncr1 mice. Growth of tumors derived from B16F10 or its knockout cell (-KO2) were monitored following subcutaneous injection in NSG mice (A: B16F10 (n = 5) or *Wisp1* KO cell (n = 5)) or in C57BL/6Ncr1 mice (B: B16F10 (n=6) or *Wisp1* KO cell (n=6)). After 21 days, remaining C57BL/6Ncr1 mice (n = 4 in each group) were euthanized and lungs and livers were assayed for B16F10 tumor cells using real time genomic qPCR, as described in Materials and Methods. (C) Representative lungs and livers from C57BL/6Ncr1 mice with B16F10 or knockout cell at day 21. (D) Real time genomic qPCR results showed quantitative tumor lung and liver metastatic burden in spontaneous metastasis assays. n.d., not detected.

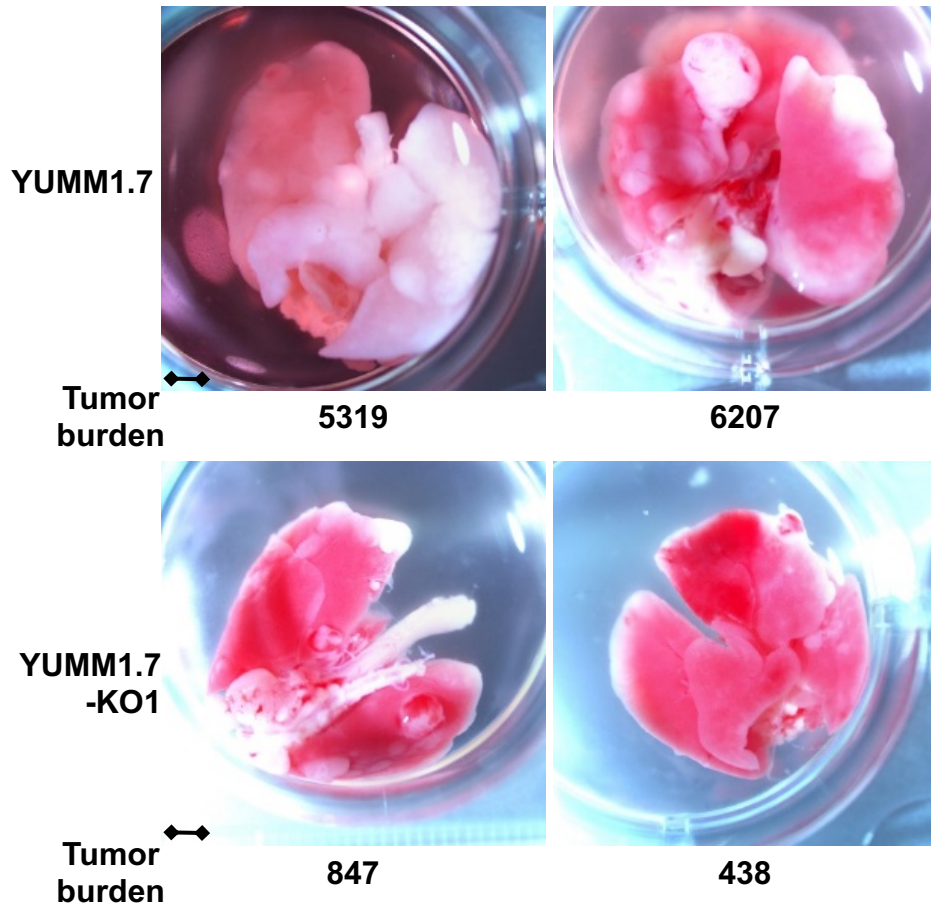
## Lung Metastasis in NSG Mice



Scale bar: 2mm; Tumor load: tumor cells in  $10^4$  lung cells

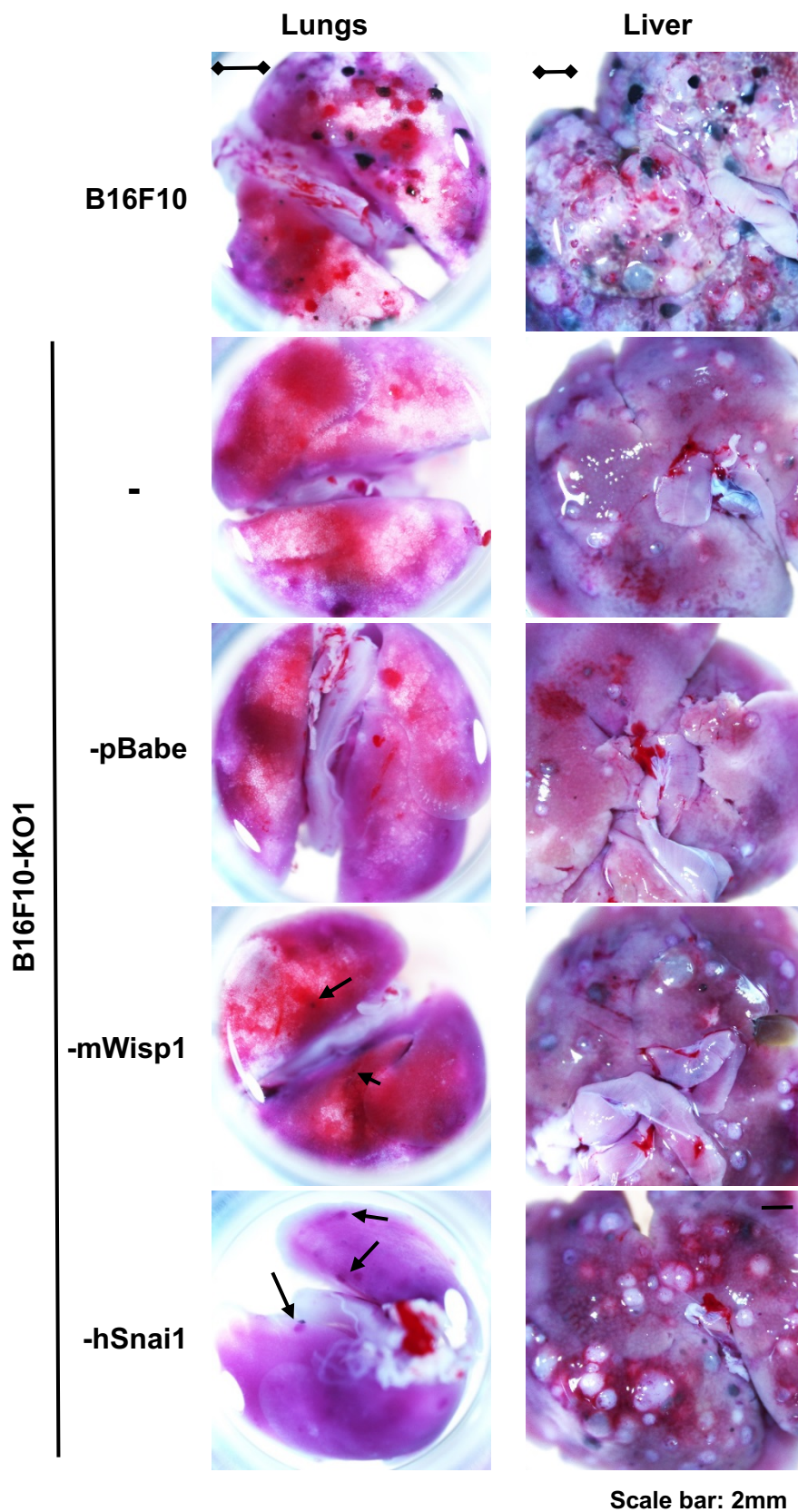
**Supplementary Figure S7.** High resolution version of Fig.4B.

## Lung Metastasis in C57 Mice



Scale bar: 2mm; Tumor load: tumor cells in  $10^4$  lung cells

**Supplementary Figure S8.** High resolution version of Fig.4F.



**Supplementary Figure S9.** High resolution version of Fig.6E.

**Supplementary Table S3.** Densitometry measurement of protein levels in Fig. 7.

**Fig.7C, B16F10/-KO1 (Lane 1-4) and YUMM1.7/-KO1 (Lane 5-8)**

Lanes	Relative Value		pAKT/AKT	Relative Value		pERK/ERK
	pAKT	AKT		pERK	ERK	
1	<b>*1.00</b>	<b>*1.00</b>	<b>1.00</b>	<b>*1.00</b>	<b>*1.00</b>	<b>1.00</b>
2	1.47	0.93	1.59	4.43	0.95	4.65
3	0.74	0.96	0.77	0.21	0.97	0.22
4	1.15	0.95	1.21	1.85	0.96	1.93
5	<b>*1.00</b>	<b>*1.00</b>	<b>1.00</b>	<b>*1.00</b>	<b>*1.00</b>	<b>1.00</b>
6	1.46	0.97	1.50	1.11	0.98	1.14
7	0.15	0.98	0.15	0.57	0.98	0.58
8	0.82	0.90	0.91	0.79	0.95	0.82

**Fig.7D, B16F10 and -KO1 (Lane 2-10)**

Lanes	Relative Value		pAKT/AKT	Relative Value		pERK/ERK
	pAKT	AKT		pERK	ERK	
1	0.33	0.52	0.63	N.A.	0.73	N.A.
2	<b>*1.00</b>	<b>*1.00</b>	<b>1.00</b>	<b>*1.00</b>	<b>*1.00</b>	<b>1.00</b>
3	1.10	1.25	0.88	0.45	1.05	0.43
4	0.99	1.15	0.86	0.90	1.12	0.81
5	1.10	1.04	1.06	0.86	0.87	0.99
6	0.98	0.96	1.03	0.25	1.08	0.23
7	0.94	0.87	1.08	0.97	1.04	0.93
8	0.66	0.78	0.84	0.61	1.00	0.60
9	0.32	0.79	0.40	0.03	1.04	0.03
10	0.81	0.83	0.97	0.37	1.01	0.36

**Fig.7E, YUMM1.7 and -KO1 (Lane 2-10)**

Lanes	Relative Value		pAKT/AKT	Relative Value		pERK/ERK
	pAKT	AKT		pERK	ERK	
1	N.A.	1.48	N.A.	0.12	1.67	0.07
2	<b>*1.00</b>	<b>*1.00</b>	<b>1.00</b>	<b>*1.00</b>	<b>*1.00</b>	<b>1.00</b>
3	0.93	0.91	1.03	1.04	1.06	0.98
4	1.02	0.88	1.16	1.00	1.07	0.94
5	0.69	1.12	0.62	0.83	1.31	0.64
6	0.26	1.03	0.25	0.87	1.24	0.70
7	0.69	0.95	0.72	0.94	1.17	0.80
8	0.29	1.01	0.29	0.63	1.21	0.52
9	0.03	0.99	0.03	0.34	0.99	0.35
10	0.23	0.75	0.30	0.51	0.86	0.59

Relative protein level was measured with Image J. In each gel, one lane from untreated wild-type cells was used as standard (relative value is 1.00) and indicated with \*.